ACCOUNTS
of chemical research

"Sticky Electrons" Transport and Interfacial Transfer of Electrons in the Dye-Sensitized Solar Cell

LAURENCE PETER*
Department of Chemistry, University of Bath, Bath BA2 7AY, United Kingdom

RECEIVED ON MAY 4, 2009

CONSPECTUS

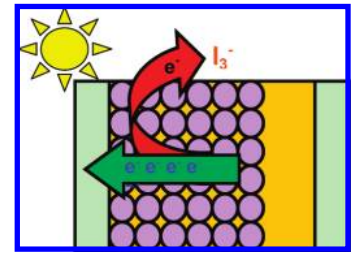

Dye-sensitized solar cells (DSCs, also known as Grätzel cells) mimic the photosynthetic process by using a sensitizer dye to harvest light energy to generate electrical power. Several functional features of these photochemical devices are unusual, and DSC research offers a rewarding arena in which to test new ideas, new materials, and new methodologies. Indeed, one of the most attractive chemical features of the DSC is that the basic concept can be used to construct a range of devices, replacing individual components with alternative materials. Despite two decades of increasing research activity, however, many aspects of the behavior of electrons in the DSC remain puzzling.

In this Account, we highlight current understanding of the processes involved in the functioning of the DSC, with particular emphasis on what happens to the electrons in the mesoporous film following the injection step. The collection of photoinjected electrons appears to involve a random walk process in which electrons move through the network of interconnected titanium dioxide nanoparticles while undergoing frequent trapping and detrapping. During their passage to the cell contact, electrons may be lost by transfer to tri-iodide species in the redox electrolyte that permeates the mesoporous film. Competition between electron collection and back electron transfer determines the performance of a DSC: ideally, all injected electrons should be collected without loss.

This Account then goes on to survey recent experimental and theoretical progress in the field, placing particular emphasis on issues that need to be resolved before we can gain a clear picture of how the DSC works. Several important questions about the behavior of "sticky" electrons, those that undergo multiple trapping and detrapping, in the DSC remain unanswered. The most fundamental of these concerns is the nature of the electron traps that appear to dominate the time-dependent photocurrent and photovoltage response of DSCs. The origin of the nonideality factor in the relationship between the intensity and the DSC photovoltage is also unclear, as is the discrepancy in electron diffusion length values determined by steady-state and non-steady-state methods. With these unanswered questions, DSC research is likely to remain an active and fruitful area for some years to come.

Introduction

The number of publications dealing with dye-sensitized solar cells (DSCs) has increased 10-fold during the past decade, with over 500 papers published in 2008 (for recent reviews, see refs 1−3). This explosion of interest stems from the pioneering work of O'Regan and Grätzel,[4] who were the first to show that efficient photoelectrochemical solar cells could be fabricated using dye-sensitized mesoporous titania films. Now, with power efficiencies over 10%, DSCs are poised for commercialization.

Figure 1 illustrates the basic principle of the DSC, which has many features in common with the photosynthetic process in plants, where coupled electron and ion fluxes are driven by the chemical energy stored in the excited states of the photosynthetic chromophores.

Typically, the light-absorbing component of the DSC is a monolayer of a ruthenium(II) bipyridyl dye[5] (or an organic dye with similar light-absorbing properties) chemisorbed on the internal surface of a ca. 10 μm thick layer of mesoporous titania on a conducting glass (or metal) substrate. This layer, consisting of interconnected nanocryst-

Published on the Web 07/28/2009 www.pubs.acs.org/acr
10.1021/ar900143m CCC: $71.50

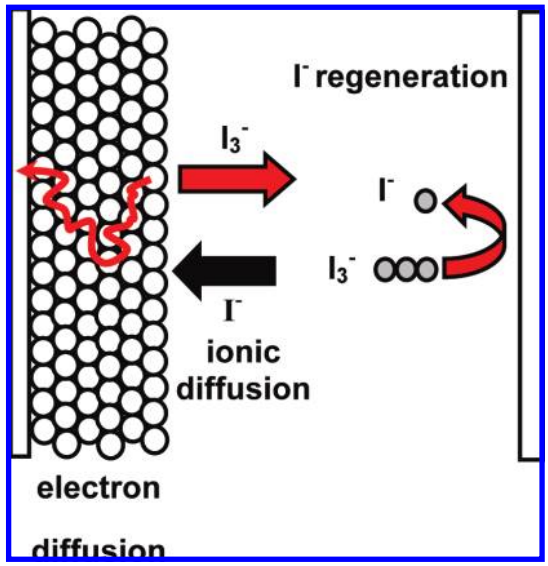

FIGURE 1. Processes taking place in a dye-sensitized solar cell under illumination. Electrons injected by photoexcited dye molecules percolate through the network of interconnected TiO_2 nanoparticles by a random walk process to the anode on the left-hand side. The electron flux in the TiO_2 is coupled to ionic fluxes in the electrolyte associated with regeneration of the dye and of iodide at the cathode on the right-hand side.

als (10−30 nm), acts as a high surface area for dye adsorption, allowing optimum light harvesting. Absorption of light by a dye molecule creates an excited molecular electronic state that rapidly injects an electron into the conduction band of the TiO_2. This charge separation step is completed on a (sub)picosecond time scale,[6,7] leaving the dye in its oxidized state. The dye is regenerated rapidly in its original oxidation state by electron transfer from iodide ions in the I_3^-/I^-redox electrolyte. The I_3^- ions formed by oxidation of I^- diffuse a short distance (<50 μm) through the electrolyte to the cathode, which is coated with a thin layer of platinum catalyst, where the regenerative cycle is completed by electron transfer to reduce I_3^- to I^-.

At first sight, the DSC appears to have little in common with conventional solid-state solar cells. Light absorption results in the formation of a localized molecular excited state rather than an electron−hole pair. Injection of an electron into the TiO_2 then leads to formation of an *electron−ion* pair. Current flow in the DSC involves diffusion of electrons in the mesoporous titania and of ions in the electrolyte, whereas the cell voltage is associated with the build up of electron concentration in the TiO_2. The porous titania layer is permeated by a concentrated redox electrolyte, so electrons and cations interact strongly over short distances, leading to coupling of electrons and ions at the nanoscopic level. As a consequence of this short-range shielding, electron transport in the TiO_2 takes place by field-free random walk[8] or ambipolar diffusion.[9]

Recombination in a solid-state solar cell involves the transition of electrons from the conduction band to the valence band, either directly or via recombination centers located in the band gap. By contrast, "recombination" in the DSC involves transfer of electrons across the oxide/electrolyte interface, either to oxidized dye molecules created by electron injection or to the oxidized component of the redox couple, that is, I_3^-. Despite these obvious differences, the thermodynamic framework describing solid-state and dye-sensitized solar cells is similar, and the current−voltage characteristics of both types of cell are described by the "diode equation",[10,11] which can be found in any standard solid-state physics textbook.[12] The reader interested in the parallels between solid-state solar cells and DSCs should consult Würfel's excellent book, *Physics of Solar Cells*.[13]

This Account highlights current understanding of the processes involved in the functioning of the DSC, with particular emphasis on what happens to the electrons in the mesoporous film following the injection step. The survey is by no means exhaustive: several aspects of the behavior of electrons in mesoporous systems remain unclear or controversial and, as a consequence, are likely to continue to stimulate fundamental research effort in the future.

The Role of Trapping in Transport and Transfer of Electrons in the DSC

Since the colloidal TiO_2 film in the DSC is annealed at high temperature to form crystalline anatase, one might expect that electrons would move through the network of interconnected nanoparticles via conduction band states, although there could be barriers between individual grains. τ_{diff}, the time taken for a free electron to diffuse across the TiO_2 film to the anode, is given by

$$\tau_{diff} = \frac{d^2}{D_0} \quad (1)$$

where d is the film thickness and D_0 is the diffusion coefficient of free electrons in the TiO_2. For $d = 10$ μm and $D_0 = 0.5$ cm^2 s^{-1} (the value for bulk anatase), electrons should reach the anode in a few microseconds. In fact, injected electrons appear to become trapped on a time scale of picoseconds to nanoseconds. In order to understand the transient photocurrent behavior of the DSC, it is necessary to decouple electron transport and interfacial transfer from the effects of trapping and detrapping of electrons. During their transit to the anode, electrons undergo multiple trapping and detrapping

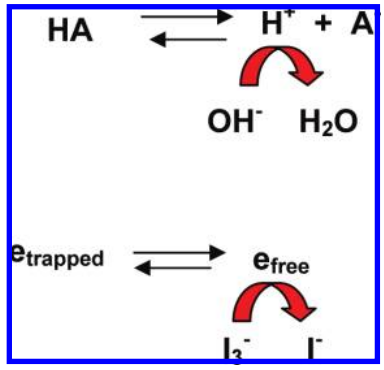

FIGURE 2. The buffering analogy. A weak acid buffers the proton concentration by dissociating during titration with an alkali. Similarly, trapped electrons in the DSC "buffer" the free electron concentration in the DSC, slowing the decay of free electron concentration during transfer to I_3^-.

(hence the title "sticky electrons"), and the photocurrent response of a DSC to a rectangular illumination pulse exhibits slow rise and fall times that range from milliseconds at high intensity to tens of seconds at low intensity. The slow rise is attributed to filling of traps and the slow fall to release of trapped electrons.[14]

Trapping/detrapping also frustrates the interpretation of time-dependent measurements aimed at quantifying the rates of electron transfer across the TiO_2 electrolyte interface, since changes in the trap occupancy occur here too. In the absence of trapping/detrapping effects, the free electron concentration following a light pulse would fall exponentially with time

$$n(t) = n(0)\, e^{-k_I I_3^- t} \qquad (2)$$

Here k_I is the rate constant for electron transfer and I_3^- is the concentration of tri-iodide ions. However, the free electron concentration in the presence of trapped electrons generally decays much slowly because the release of trapped electrons to the conduction band effectively "buffers" the free electron concentration. This buffering of the free electron concentration by trapped electrons effect is analogous to the buffing of proton concentration by a weak acid, as illustrated in Figure 2.

Kinetics of Injection and Back Transfer of Electrons in the DSC

Under steady-state illumination, the rates of trapping and detrapping of electrons in the DSC must be equal because the local electron concentration does not vary with time. If the cell is illuminated at open circuit under steady-state conditions, no current is extracted from the cell. The injected electron flux must therefore be balanced by electron transfer back to the oxidized dye (D^+) or to I_3^- (eqs 5 and 7).

$$D + h\upsilon \rightarrow D^* \qquad \text{photoexcitation} \qquad (3)$$

$$D^* \rightarrow D^+ + e^-_{TiO_2} \qquad \text{electron injection} \qquad (4)$$

$$D^+ + e^-_{TiO_2} \xrightarrow{k_D} D \qquad \text{back transfer of electrons to } D^+ \qquad (5)$$

$$2D^+ + 3I^- \xrightarrow{k_R} D + I_3^- \qquad \text{regeneration of dye by iodide} \qquad (6)$$

$$I_3^- + 2e^-_{TiO_2} \xrightarrow{k_I} 3I^- \qquad \text{back transfer of electrons to } I_3^- \qquad (7)$$

These processes are illustrated schematically in Figure 3.

In an efficient DSC, dye regeneration (reaction 6) needs to be fast in order to prevent loss of electrons by reaction 5. However, transfer of electrons to I_3^- (reaction 7) needs to be slow so that electrons can build up in the TiO_2 to produce a photovoltage. Haque et al.[15] have used transient absorbance measurements in the absence of I_3^- to show that the rate of reaction 5 depends strongly on the concentration of electrons in the TiO_2. These authors demonstrated that reaction 5 became faster than reaction 6 at negative applied voltages where electrons build up in the oxide, reducing the half-life for the decay of the D^+ absorbance to less than 30 ns. Back electron transfer to D^+ may therefore limit cell performance at high light intensities where regeneration of the dye via reaction 6 fails to compete effectively with reaction 5.

An order of magnitude estimate of the upper limit of k_D can be obtained by assuming that the rate of reaction 5 is limited by the rate of electron diffusion in the mesoporous oxide, when

$$k_D = 4\pi D_0 r_{eD} \qquad (8)$$

where r_{eD} represents the distance of closest approach of the electron to D^+. Using the diffusion coefficient for free electrons in crystalline anatase (0.5 $cm^2\ s^{-1}$) and $r_{eD} = 0.2$ nm gives $k_D \approx 10^{-7}\ cm^3\ s^{-1}$. This corresponds to a lower limit for the D^+ half-life of 1 ns when the free electron density reaches $10^{16}\ cm^{-3}$.

A similar order of magnitude estimate of the upper limit of k_R, the rate constant for dye regeneration by iodide, can be made by assuming that the process is limited by diffusion of I^- ions. In eq 8, D_0 is replaced by D_{I^-} (typically $\sim 10^{-6}\ cm^2\ s^{-1}$) and r_{eD} by a similar value for the D^+/I^- separation, giving $k_R \approx 10^{-13}\ cm^{-3}\ s^{-1}$. Since the concentration of iodide ions (0.5 M $\equiv 3 \times 10^{20}\ cm^{-3}$) is much higher than that of D^+, the reaction is expected to be pseudo-first-order with a rate constant $k_R I^- \approx 3 \times 10^7\ s^{-1}$, corresponding to regeneration of the dye on a submicrosecond time scale (half-life of 30 ns). This is

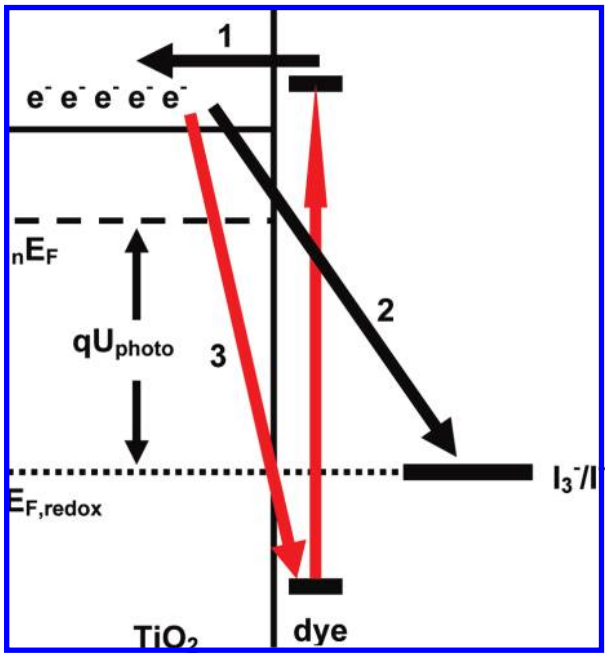

FIGURE 3. The DSC under illumination at open circuit. The photovoltage, which corresponds to the difference between the electron quasi-Fermi level in the TiO_2 and the redox Fermi level, depends on the balance between injection into the conduction band (1) and back transfer (2, 3) of electrons. To achieve high voltages, processes 2 and 3 need to be as slow as possible.

somewhat faster than the shortest half-life values reported in the literature.[16]

By contrast with rapid dye regeneration or electron transfer to D^+, electron transfer to I_3^- is slow, since it involves breaking the iodine−iodine bond (this contrasts with the rapid electron transfer to I_3^- that occurs at the platinum coated cathode, where the I−I bond is broken by chemisorption). Measurement of the rate of electron transfer to I_3^- is complicated by the effects of electron trapping/detrapping, but an order of magnitude estimate[1] for $k_I I_3^-$ is 10^3−10^4 s^{-1}. Slow electron transfer from the TiO_2 to the redox couple (i.e., a long electron lifetime) is needed for efficient operation of the DSC, since the generation of a voltage relies on a substantial build up of electron concentration in the TiO_2. Gregg et al.[17] have shown that the DSC photovoltage almost disappears when the slow I_3^-/I^- redox couple is replaced by the fast outer-sphere ferrocinium/ferrocene redox couple. However, this does not mean that the I_3^-/I^- couple is necessarily unique: it has been replaced successfully by a cobalt-based redox system,[18] as well as by organic hole conductors.[19]

What Determines the Photovoltage in a DSC?

The photovoltage in a solar cell corresponds to the difference in the *Fermi energy*, E_F, of electrons in the two contacts. At equilibrium in the dark, E_F, must be the same in all phases in the DSC and equal to $E_{F,redox}$, the I_3^-/I^- Fermi level. Under illumination at open circuit, the concentration of electrons in the TiO_2 increases to a stationary value determined by the balance between electron injection and electron transfer to I_3^- and the oxidized dye. At 1 sun, for example, the electron injection rate is on the order of 10^{20} cm^{-3} s^{-1}. If the free electron lifetime is 10^{-4} s, the steady-state free electron concentration will be $10^{20} \times 10^{-4} = 10^{16}$ cm^{-3}. This steady-state electron concentration defines ${}_nE_F$, the *quasi-Fermi level* (QFL) of electrons. The photovoltage, which corresponds to the increase in Fermi level, therefore depends on the rate at which electrons escape from the TiO_2: achievement of high photovoltages requires slow back transfer to I_3^-.

U_{photo}, the photovoltage of the DSC is determined by the ratio of the values of free electron concentration in the TiO_2 in the dark and under illumination.

$$U_{photo} = \frac{1}{q}({}_nE_F - E_{F,redox}) = \frac{k_B T}{q} \ln \frac{n_{light}}{n_{dark}} \quad (9)$$

where n_{dark} is related to $E_{F,redox}$ by

$$n_{dark} = N_C \exp -\left(\frac{E_C - E_{F,redox}}{k_B T}\right) \quad (10)$$

N_C is the density of conduction band states in the TiO_2, and E_C is the conduction band energy. n_{light} is related to the QFL, ${}_nE_F$, by

$$n_{light} = N_C \exp -\left(\frac{E_C - {}_nE_F}{k_B T}\right) \quad (11)$$

Equation 9 predicts that U_{photo} should increase by 59 mV for every 10-fold increase in the ratio n_{light}/n_{dark} at room temperature. Typical DSC voltages under 1 sun illumination are in the range 0.7−0.8 V, corresponding to $n_{light}/n_{dark} = 10^{12}$−$10^{13}$. The electron concentration in the dark is extraordinarily low in the DSC (below 10^4 cm^{-3}, that is, only 10 electrons cm^{-2} in a 10 μm thick TiO_2 film!) because it is determined by equilibration with the I_3^-/I^- redox system, which effectively removes electrons from the TiO_2 ($E_{F,redox}$ is believed to be around 1 eV below E_C).

Nonideality

If recombination of electrons with D^+ is negligible, the intensity dependence of the DSC photovoltage should be given by

$$\frac{dU_{photo}}{d\log_{10} I_0} = 2.303\frac{kT}{q} \quad (12)$$

corresponding to the slope of 59 mV/decade in a plot of U_{photo} vs, $\log_{10}$(intensity). However, most DSCs are not ideal: gener-

ally U_{photo} increases by more than 59 mV/decade, and values as large as 120 mV/decade are not uncommon. Nonideal behavior can be dealt with empirically by introducing an ideality factor $m > 1$ into the numerator of the right-hand term in eq 12, so that for $m = 2$, for example, the slope becomes 118 mV/decade.

The origin of nonideality in DSCs is not well understood. There are several possible explanations. One is that electron transfer from the TiO_2 layer to I_3^- ions takes place via "surface states", surface energy levels located in some kind of energy distribution below the conduction band.[20] If surface states do mediate electron transfer, removing them or passivating them should improve the photovoltage. This could be a fruitful area for further experiments. However, DSCs also appear to behave nonideally at short circuit, when photoinjected electrons are collected at the anode.[21] Electron transfer to I_3^- via surface states cannot be responsible in this case, raising the question whether the behavior of electrons in a mesoporous film permeated by electrolyte is intrinsically nonideal. Under 1 sun illumination, high total electron concentrations up to 10^{19} cm^{-3} can be reached, corresponding to 10−100 electrons per particle and an average electron−electron distance of 5 nm or less. Coulombic trapping of electrons near the interface between the TiO_2 particles and the adjacent ionic solution could result in formation a nonideal 2-D electron gas with strong electron−electron repulsions of the kind seen at semiconductor surfaces under inversion conditions. It is possible, therefore, that the "electron traps" discussed in the DSC literature may not be physical defects in the TiO_2 but rather a manifestation of Coulombic trapping. The consequences of these interactions for the dependence of the electron Fermi level on electron concentration remain to be explored; it may be necessary to introduce an activity coefficient to describe the nonideality of the electron gas. The lack of understanding in this area highlights the need for theoretical modeling of nanostructured systems with two intimately mixed phases with high charge density.

Transport and Transfer of Electrons in the DSC: The Continuity Equation

The fate of photoinjected electrons in the DSC is described by the time-dependent *continuity equation*. For illumination through the anode side of the DSC, this takes the form[21]

$$\frac{\partial n_c}{\partial t} = \alpha I_0 \exp(-\alpha x) - N_{t,0}\left\langle \frac{\partial f}{\partial t} \right\rangle + D_0 \frac{\partial^2 n_c}{\partial x^2} - \frac{(n_c - n_{eq})}{\tau_0} \quad (13)$$

n_c is the concentration of electrons in the conduction band, α is the wavelength-dependent absorption coefficient of the dye-sensitized layer (determined by the loading and molar absorption coefficient of the sensitizer dye), x is the distance from the anode, I_0 is the incident photon flux (corrected for reflection and absorption losses), $N_{t,0}$ is the concentration of electron traps, f is the probability of trap occupation, D_0 is the diffusion coefficient of conduction band electrons, n_{eq} is the equilibrium concentration of electrons in the conduction band (i.e., in the dark at open circuit), and τ_0 is the electron lifetime defined by $\tau_0 = 1/k[I_3^-]$ (cf. eq 2). The first term on the right-hand side represents the local electron injection rate (assuming 100% injection efficiency), the second term describes electron trapping/detrapping averaged over the trap state energies, the third term describes the time-dependent diffusion of free electrons, and the final term describes the loss of electrons by back reaction with tri-iodide.

The continuity equation can be solved for steady-state conditions[13] ($\partial f/\partial t = 0$) as well as for different perturbations. Figure 4a contrasts the steady-state profiles of conduction band electrons calculated for open circuit and short circuit. Figure 4b illustrates the corresponding quasi-Fermi level profiles (cf. eq 11). It can be seen that the quasi-Fermi level drops steeply close to the anode under short circuit conditions, whereas it is flat in the open circuit case.

The validity of the calculations shown in Figure 4 has been tested by constructing a DSC in which the Fermi level at the electrolyte side of the film was measured using an evaporated titanium contact.[22] The results indicate that the steady-state solution of the continuity equation correctly predicts the Fermi level over the entire current−voltage characteristic of the DSC. A similar type of cell has also been used to investigate how the Fermi level varies with temperature.[23]

Collecting Electrons: The Electron Diffusion Length

Competition between electron transport to the anode and loss by transfer to I_3^- can be expressed in terms of the electron diffusion length, $L_0 = (D_0\tau_0)^{1/2}$, which appears in the solutions of the steady-state continuity equation given originally by Sodergren et al.[11] L_0 is an important figure of merit for DSCs since it is a measure of how far an electron diffuses toward the anode before it is lost by electron transfer to I_3^-. Figure 5 shows how the efficiency of electron collection depends on the ratio of L_0 to the film thickness d for illumination from the anode substrate side (SE) and from the electrolyte side (EE). It can be seen that efficient collection requires L_0/d to be greater than 2.

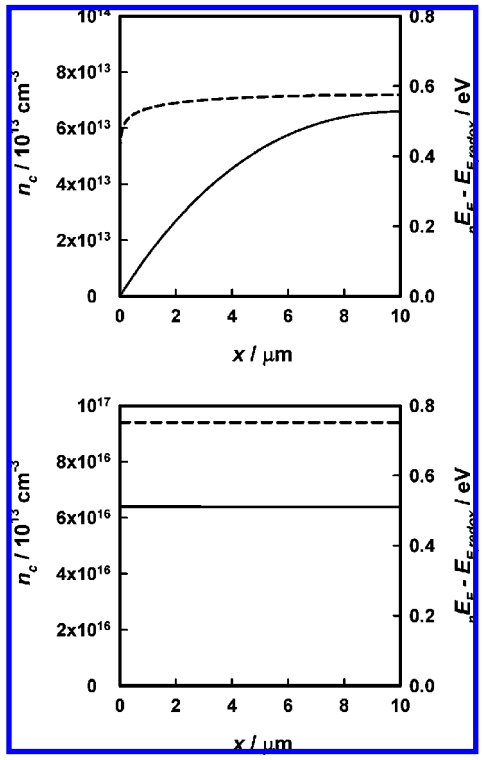

FIGURE 4. (a) Typical concentration profile of free electrons in the DSC under short circuit conditions calculated from the continuity equation. The broken line shows the corresponding variation of the quasi-Fermi level in the oxide (relative to the redox Fermi level, $E_{F,redox}$). Values used in calculation: $N_C = 10^{21}$ cm^{-3}, $D_0 = 0.4$ cm^2 s^{-1}, $\tau_0 = 10^{-3}$ s, incident photon flux $= 10^{17}$ cm^{-2} s^{-1}. (b) Typical free electron concentration profile in the DSC at open circuit and the corresponding quasi-Fermi level relative to the redox Fermi level (broken line, compare with Figure 7a). The photovoltage corresponds to the difference between the quasi-Fermi level of electrons in the TiO_2 and the redox Fermi level.

Figure 5 shows that that the ratio of the collection efficiency for SE and EE illumination is sensitive to the value of L_n/d. This is the basis for a steady-state method for the determination of

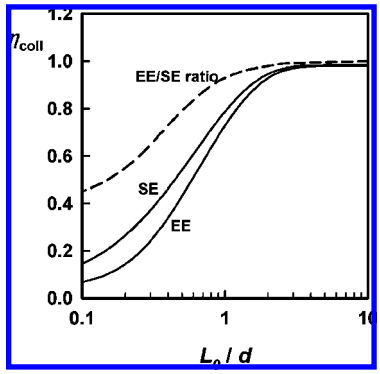

FIGURE 5. Electron collection efficiency calculated from the continuity equation as a function of the ratio of the steady-state electron diffusion length L_0 to the TiO_2 film thickness d for illumination from the substrate side (SE) and from the electrolyte side (EE). $\alpha = 10^3$ cm^{-1}; $d = 10$ μm. The EE/SE ratio can be used to determine the value of L_0.

L_0 originally described by Södergren et al.[11] and discussed recently by Halme at al.[24] and by Barnes et al.[25] The interested reader is referred to these papers for details of the spectral analysis. Good DSCs are generally characterized by L_0 values that are 2−3 times the film thickness.

Time-Dependent Response of the DSC: Determination of D_n and τ_n

Solutions of the time-dependent continuity equation for non-steady-state conditions can be obtained numerically.[21] However, the trapping term was omitted in early work,[26] where the continuity equation was solved analytically for small amplitude perturbations using intensity dependent *effective* values of the electron diffusion coefficient (D_n) and electron lifetime (τ_n) rather than the corresponding free electron values D_0 and τ_0. It has been observed that D_n increases with intensity, whereas τ_n decreases with intensity in such a way that the product $D_n\tau_n$ is almost independent of intensity.[27] The intensity dependence of D_n and τ_n is believed to arise from relaxation of the concentration of trapped electrons, which are exchanged with mobile electrons in the conduction band. The time constant for this relaxation has been discussed by Bisquert and Vikhrenko[28] within the framework of the *quasi-static approximation*. Their treatment shows that the effective diffusion coefficient and effective electron lifetime depend on trap occupancy and hence on the Fermi level. The quasi-static approximation predicts that the effective electron lifetime τ_n, is given by

$$\tau_n = \left(1 + \frac{\partial n_t}{\partial n_c}\right)\tau_0 \qquad (14)$$

whereas the effective electron diffusion coefficient D_n is given by

$$D_n = \left(1 + \frac{\partial n_t}{\partial n_c}\right)^{-1} D_0 \qquad (15)$$

The $\partial n_t/\partial n_c$ term and its inverse reflect the way that the densities of trapped and free electrons (n_t and n_c respectively) vary with changes in the quasi-Fermi level. This variation is the product of two terms:

$$\frac{\partial n_t}{\partial n_c} = \frac{\partial n_t}{\partial {}_nE_F}\frac{\partial {}_nE_F}{\partial n_c} = g({}_nE_F)\frac{k_BT}{n_c} \qquad (16)$$

where $g({}_nE_F)$ is the density of states function for the trap states. The experimentally observed power law intensity dependence of D_n and τ_n illustrated in Figure 6 can be rationalized if the electron trap distribution is exponential with the form

$$g[E_t] = \frac{N_{t,0}}{k_B T_0} \exp -\left[\frac{E_c - E_t}{k_B T_0}\right] \qquad (17)$$

where N_t is the total trap concentration (typically $10^{19}-10^{20}$ cm^{-3}) and T_0 is a characteristic temperature that is generally found to be considerably higher than ambient temperature (T_0 = 600−1500 K).[29] The effective electron lifetime decreases as the bias light intensity increases, since n_c varies more rapidly with ${}_nE_F$ than $g({}_nE_F)$ if the characteristic temperature of the trap distribution (T_0) is greater than the ambient temperature (T). The effective diffusion coefficient caries in the opposite sense for the same reason as shown in Figure 6.

Time-dependent techniques are generally based on two types of perturbation. The first type uses a time-dependent illumination signal to change the rate of electron injection into the mesoporous oxide. The perturbation can be large (usually starting from an initial dark condition), or it can be a small in amplitude and superimposed on steady background illumination (this has the advantage of linearizing the system response). The perturbation can be a short laser pulse, a rectangular light pulse, or a sinusoidal intensity profile (as in intensity modulated photocurrent and photovoltage spectroscopy, IMPS and IMVS, respectively). The photocurrent response of the DSC is normally measured for perturbation under short circuit conditions, whereas the photovoltage response is measured at open circuit. IMPS[26] and IMVS[30] are small amplitude techniques. An example of a large amplitude technique is photovoltage decay,[31,32] which gives information about τ_n and the trap distribution. An example of the use of IMPS and IMVS to determine the D_n and τ_n, respectively, as a function of illumination intensity is illustrated in Figure 7.

The second type of perturbation involves modulating the voltage applied to a DSC, either in the dark or under illumination. This is the basis for impedance measurements, which are increasingly being used to characterize DSCs.[33,34] All of these techniques measure the *effective* values D_n and τ_n rather than D_0 and τ_0. When D_n is measured at short circuit and τ_n at open circuit, calculation of the electron diffusion length is complicated by the fact that the trap occupancy is different in the two cases.[9] Two techniques that allow measurement of D_n and τ_n for the same trap occupancy are impedance measurements under illumination at open circuit and small amplitude photovoltage rise and decay time measurements at open circuit, an ingenious method proposed by O'Regan et al.[35]

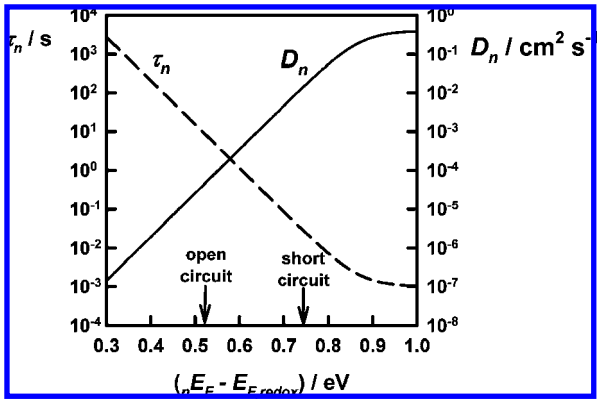

FIGURE 6. Dependence of the effective values of electron lifetime and electron diffusion coefficient on the electron quasi-Fermi level predicted by the quasi-static approach. Values used in calculation: $N_C = 10^{21}$ cm^{-3}; $N_{t,0} = 10^{20}$ cm^{-3}; $T_0 = 1000$ K; $D_0 = 0.4$ cm^2 s^{-1}; $\tau_0 = 10^{-3}$ s. See ref 1 for further details.

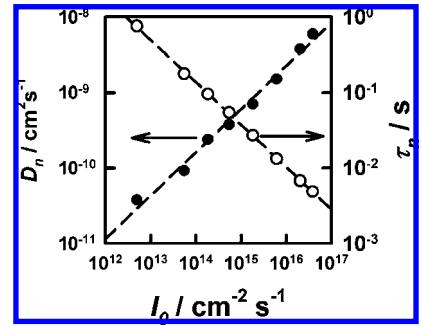

FIGURE 7. Experimentally determined intensity dependence of D_n and τ_n showing typical power law behavior arising from trapping/detrapping for an exponential distribution of trap states. Note that the product $D_n\tau_n$ is almost independent of intensity.

According to the analysis given by Bisquert and Vikhrenko,[28] the equality $(D_0\tau_0)^{1/2} = (D\tau_n)^{1/2}$ holds only when D_n and τ_n are measured *at the same trap occupancy*. This approach has been used in a number of studies,[36,37] but it is worth noting that the electron diffusion lengths obtained by non-steady-state methods are generally higher than those found by the analysis of IPCE spectra for EE and SE illumination.[24,25] This discrepancy needs further investigation.

Investigations of Electron Trapping in DSCs

The increase in the concentration of trapped electrons in the DSC as the Fermi level moves toward the conduction band corresponds to a chemical capacitance[3,38] that can be measured by impedance spectroscopy. Integration of this capacitance gives the total trapped charge electron concentration as a function of ${}_nE_F - E_{F,redox}$. Trapped electrons present at open circuit can be extracted by short circuiting the cell; integration of the resulting current transient gives the trapped charge: this is the basis of the charge extraction method.[29,39] A simpler approach is to use near-IR absorbance measurements to follow changes in the trapped electron concentration.[40] Figure 8 illustrates the changes in near-IR transmittance when a DSC is illuminated at open circuit. Frequency-resolved IR transmittance measurements

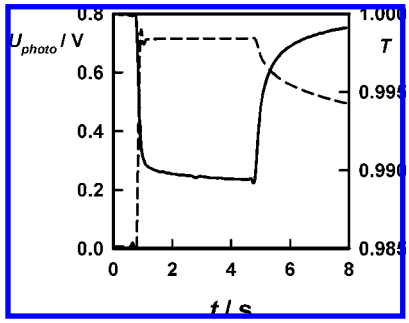

FIGURE 8. Response of IR transmittance and photovoltage (broken line) of a dye-sensitized solar cell to a square wave illumination pulse. The light was switched on after ~1 s and off after 5 s. The absorbance arises from trapped electrons.

have also been used to study the dynamics of electrons in DSCs under different conditions.[41]

Further work is needed to determine whether the density and energetic distribution of electron traps is an intrinsic property of the oxide or whether it also depends on factors such as the composition and ionic strength of the electrolyte phase, as might be expected if trapping is due to electron−ion interactions rather than defect states in the oxide.

Conclusions

Although considerable progress has been made in the past decade, this brief survey suggests that several important questions about the behavior of "sticky" electrons in the DSC remain unanswered. Probably the most fundamental of these concerns the nature of the electron traps that appear to dominate the time-dependent photocurrent and photovoltage response of DSCs. The origin of the nonideality factor also remains to be clarified, as does the discrepancy in electron diffusion length values determined by steady-state and nonsteady-state methods.

The author thanks present and past members of his research group as well as Alison Walker (Department of Physics, University of Bath), who have all contributed to the understanding of DSCs. Financial support for this work has been provided by the UK Engineering and Physical Science Research Council (EPSRC).

BIOGRAPHICAL INFORMATION

Laurie Peter received his B.Sc. and Ph.D. from the University of Southampton (U.K.). After a period working at the Fritz Haber Institute in Berlin, he returned to Southampton before moving to the University of Bath, where he has been Professor of Physical Chemistry since 1993.

FOOTNOTES

*E-mail: l.m.peter@bath.ac.uk.

REFERENCES

1 Peter, L. M. Characterization and modeling of dye-sensitized solar cells. *J. Phys. Chem. C* **2007**, *111*, 6601–6612.
2 Peter, L. M. Dye-sensitized nanocrystalline solar cells. *Phys. Chem. Chem. Phys.* **2007**, *9*, 2630–2642.
3 Bisquert, J.; Cahen, D.; Hodes, G.; Ruhle, S.; Zaban, A. Physical chemical principles of photovoltaic conversion with nanoparticulate, mesoporous dye-sensitized solar cells. *J. Phys. Chem. B* **2004**, *108*, 8106–8118.
4 O'Regan, B.; Gratzel, M. A low-cost, high-efficiency solar-cell based on dye-sensitized colloidal TiO_2 Films. *Nature* **1991**, *353*, 737–740.
5 Nazeeruddin, M. K.; Klein, C.; Liska, P.; Gratzel, M. Synthesis of novel ruthenium sensitizers and their application in dye-sensitized solar cells. *Coord. Chem. Rev.* **2005**, *249*, 1460–1467.
6 Rehm, J. M.; McLendon, G. L.; Nagasawa, Y.; Yoshihara, K.; Moser, J.; Gratzel, M. Femtosecond electron-transfer dynamics at a sensitizing dye−semiconductor (TiO_2) interface. *J. Phys. Chem.* **1996**, *100*, 9577–9578.
7 Tachibana, Y.; Nazeeruddin, M. K.; Gratzel, M.; Klug, D. R.; Durrant, J. R. Electron injection kinetics for the nanocrystalline TiO_2 films sensitised with the dye $(Bu_4N)_2Ru(dcbpyH)_2(NCS)_2$. *Chem. Phys.* **2002**, *285*, 127–132.
8 Nelson, J. Continuous-time random-walk model of electron transport in nanocrystalline TiO_2 electrodes. *Phys. Rev. B* **1999**, *59*, 15374–15380.
9 Kopidakis, N.; Schiff, E. A.; Park, N. G.; van de Lagemaat, J.; Frank, A. J. Ambipolar diffusion of photocarriers in electrolyte-filled, nanoporous TiO_2. *J. Phys. Chem. B* **2000**, *104*, 3930–3936.
10 Sze S. M. *Physics of Semiconductor Devices*, 2nd ed.; John Wiley & Sons, Inc: New York, 1981.
11 Södergren, S.; Hagfeldt, A.; Olsson, J.; Lindquist, S. E. Theoretical models for the action spectrum and the current-voltage characteristics of microporous semiconductor films in photoelectrochemical cells. *J. Phys. Chem.* **1994**, *98*, 5552–5555.
12 Sze, S. M. *Semiconductor devices physics and technology*; Wiley: New York, 1985.
13 Wurfel, P. *Physics of Solar Cells*; Wiley-VCH: Weinheim, Germany, 2005.
14 Walker, A. B.; Peter, L. M.; Martinez, D.; Lobato, K. Transient photocurrents in dye-sensitized nanocrystalline solar cells. *Chimia* **2007**, *61*, 792–795.
15 Haque, S. A.; Tachibana, Y.; Klug, D. R.; Durrant, J. R. Charge recombination kinetics in dye-sensitized nanocrystalline titanium dioxide films under externally applied bias. *J. Phys. Chem. B* **1998**, *102*, 1745–1749.
16 Montanari, I.; Nelson, J.; Durrant, J. R. Iodide electron transfer kinetics in dye-sensitized nanocrystalline TiO_2 films. *J. Phys. Chem. B* **2002**, *106*, 12203–12210.
17 Gregg, B. A.; Pichot, F.; Ferrere, S.; Fields, C. L. Interfacial recombination processes in dye-sensitized solar cells and methods to passivate the interfaces. *J. Phys. Chem. B* **2001**, *105*, 1422–1429.
18 Nusbaumer, H.; Zakeeruddin, S. M.; Moser, J. E.; Gratzel, M. An alternative efficient redox couple for the dye-sensitized solar cell system. *Chem.—Eur. J.* **2003**, *9*, 3756–3763.
19 Kruger, J.; Plass, R.; Cevey, L.; Piccirelli, M.; Gratzel, M.; Bach, U. High efficiency solid-state photovoltaic device due to inhibition of interface charge recombination. *Appl. Phys. Lett.* **2001**, *79*, 2085–2087.
20 Salvador, P.; Hidalgo, M. G.; Zaban, A.; Bisquert, J. Illumination intensity dependence of the photovoltage in nanostructured TiO_2 dye-sensitized solar cells. *J. Phys. Chem. B* **2005**, *109*, 15915–15926.
21 Jennings, J. R.; Ghicov, A.; Peter, L. M.; Schmuki, P.; Walker, A. B. Dye-sensitized solar cells based on oriented TiO2 nanotube arrays: Transport, trapping, and transfer of electrons. *J. Am. Chem. Soc.* **2008**, *130*, 13364–13372.
22 Lobato, K.; Peter, L. M.; Wurfel, U. Direct measurement of the internal electron quasi-Fermi level in dye sensitized solar cells using a titanium secondary electrode. *J. Phys. Chem. B* **2006**, *110*, 16201–16204.
23 Lobato, K.; Peter, L. M. Direct measurement of the temperature coefficient of the electron quasi-Fermi level in dye-sensitized nanocrystalline solar cells using a titanium sensor electrode. *J. Phys. Chem. B* **2006**, *110*, 21920–21923.
24 Halme, J.; Boschloo, G.; Hagfeldt, A.; Lund, P. Spectral characteristics of light harvesting, electron injection, and steady-state charge collection in pressed TiO_2 dye solar cells. *J. Phys. Chem. C* **2008**, *112*, 5623–5637.
25 Barnes, P. R. F.; Anderson, A. Y.; Koops, S. E.; Durrant, J. R.; O'Regan, B. C. Electron injection efficiency and diffusion length in dye-sensitized solar cells derived from incident photon conversion efficiency measurements. *J. Phys. Chem. C* **2009**, *113*, 1126–1136.
26 Dloczik, L.; Ileperuma, O.; Lauermann, I.; Peter, L. M.; Ponomarev, E. A.; Redmond, G.; Shaw, N. J.; Uhlendorf, I. Dynamic response of dye-sensitized nanocrystalline

solar cells: Characterization by intensity-modulated photocurrent spectroscopy. *J. Phys. Chem. B* **1997**, *101*, 10281–10289.

27 Fisher, A. C.; Peter, L. M.; Ponomarev, E. A.; Walker, A. B.; Wijayantha, K. G. U. Intensity dependence of the back reaction and transport of electrons in dye-sensitized nanacrystalline TiO_2 solar cells. *J. Phys. Chem. B* **2000**, *104*, 949–958.

28 Bisquert, J.; Vikhrenko, V. S. Interpretation of the time constants measured by kinetic techniques in nanostructured semiconductor electrodes and dye-sensitized solar cells. *J. Phys. Chem. B* **2004**, *108*, 2313–2322.

29 Bailes, M.; Cameron, P. J.; Lobato, K.; Peter, L. M. Determination of the density and energetic distribution of electron traps in dye-sensitized nanocrystalline solar cells. *J. Phys. Chem. B* **2005**, *109*, 15429–15435.

30 Schlichthorl, G.; Park, N. G.; Frank, A. J. Evaluation of the charge-collection efficiency of dye-sensitized nanocrystalline TiO_2 solar cells. *J. Phys. Chem. B* **1999**, *103*, 782–791.

31 Bisquert, J.; Zaban, A.; Greenshtein, M.; Mora-Sero, I. Determination of the rate constants for charge transfer and the distribution of semiconductor and electrolyte electronic energy levels in dye-sensitized solar cells by open circuit photovoltage decay method. *J. Am. Chem. Soc.* **2004**, *126*, 13550–13569.

32 Walker, A. B.; Peter, L. M.; Lobato, K.; Cameron, P. J. Analysis of photovoltage decay transients in dye-sensitized solar cells. *J. Phys. Chem. B* **2006**, *110*, 25504–25507.

33 Fabregat-Santiago, F.; Bisquert, J.; Palomares, E.; Otero, L.; Kuang, D. B.; Zakeeruddin, S. M.; Gratzel, M. Correlation between photovoltaic performance and impedance spectroscopy of dye-sensitized solar cells based on ionic liquids. *J. Phys. Chem. C* **2007**, *111*, 6550–6560.

34 Wang, Q.; Moser, J. E.; Gratzel, M. Electrochemical impedance spectroscopic analysis of dye-sensitized solar cells. *J. Phys. Chem. B* **2005**, *109*, 14945–14953.

35 O'Regan, B. C.; Bakker, K.; Kroeze, J.; Smit, H.; Sommeling, P.; Durrant, J. R. Measuring charge transport from transient photovoltage rise times. A new tool to investigate electron transport in nanoparticle films. *J. Phys. Chem. B* **2006**, *110*, 17155–17160.

36 Jennings, J. R.; Peter, L. M. A reappraisal of the electron diffusion length in solid-state dye-sensitized solar cells. *J. Phys. Chem. C* **2007**, *111*, 16100–16104.

37 Dunn, H. K.; Peter, L. M. How efficient is electron collection in dye-sensitized solar cells? Comparison of different dynamic methods for the determination of the electron diffusion length. *J. Phys. Chem. C* **2009**, *113*, 4726–4731.

38 Bisquert, J. Chemical capacitance of nanostructured semiconductors: its origin and significance for nanocomposite solar cells. *Phys. Chem. Chem. Phys.* **2003**, *5*, 5360–5364.

39 Duffy, N. W.; Peter, L. M.; Rajapakse, R. M. G.; Wijayantha, K. G. U. A novel charge extraction method for the study of electron transport and interfacial transfer in dye sensitised nanocrystalline solar cells. *Electrochem. Commun.* **2000**, *2*, 658–662.

40 Nguyen, T. T. O.; Peter, L. M.; Wang, H. Characterization of electron trapping in dye-sensitized solar cells by near-IR transmittance measurements. *J. Phys. Chem. C* **2009**, *113*, 8532–8536.

41 Franco, G.; Gehring, J.; Peter, L. M.; Ponomarev, E. A.; Uhlendorf, I. Frequency-resolved optical detection of photoinjected electrons in dye-sensitized nanocrystalline photovoltaic cells. *J. Phys. Chem. B* **1999**, *103*, 692–698.